

Reactive Ce_{0.8}RE_{0.2}O_{1.9} (RE = La, Nd, Sm, Gd, Dy, Y, Ho, Er, and Yb) Powders via Carbonate Coprecipitation. 2. Sintering

Ji-Guang Li,* Takayasu Ikegami, Toshiyuki Mori, and Toshiaki Wada

National Institute for Research in Inorganic Materials,[†] Namiki 1-1, Tsukuba, Ibaraki 305-0044, Japan

Received February 21, 2001. Revised Manuscript Received June 5, 2001

The densification behavior of nanocrystalline Ce_{0.8}RE_{0.2}O_{1.9} (RE = La, Nd, Sm, Gd, Dy, Y, Ho, Er, and Yb) solid-solution oxides, synthesized via carbonate coprecipitation, has been investigated in air by means of constant-rate-of-heating sintering and the conventional ramp-and-holding sintering methods. Fully dense Ce_{0.8}RE_{0.2}O_{1.9} ceramics with ultrafine microstructures (grain size ≈150–250 nm) were obtained at very low sintering temperatures of 1100–1250 °C from the powders calcined at 700 °C. The effect of calcination temperature on the sinterability of Ce_{0.8}RE_{0.2}O_{1.9} oxides was discussed using three typical samples: Ce_{0.8}-La_{0.2}O_{1.9}, Ce_{0.8}Sm_{0.2}O_{1.9}, and Ce_{0.8}Yb_{0.2}O_{1.9}. The densification behavior of Ce_{0.8}RE_{0.2}O_{1.9} materials was found to mainly depend on powder characteristics, that is, the rate of crystallite coarsening upon calcination, particle morphology, and the extent of agglomeration.

Introduction

Cerium dioxide doped with ≈20 at. % of various rare-earth (RE) cations (hereafter referred to as 20REDC) shows a higher oxygen ion conductivity than yttria-stabilized zirconia and has been considered a promising electrolyte material for solid oxide fuel cells (SOFCs) and as oxygen sensors.^{1,2} From the viewpoint of long-term applications, the electrolyte material should have nearly full density, uniform microstructure, homogeneous composition, and high purity. Nearly complete densification is needed to avoid possible changes in the electrical properties arising from rearrangement or elimination of pores during prolonged anneals at the operating temperature. While uniform microstructure and homogeneous composition are required so that the material would exhibit a simple and interpretable ac response both for the intrinsic impedance of the grains and for the grain boundary impedance. To achieve these goals, the 20REDC solid-solution powders produced by the solid-state reaction method have to be densified at temperatures as high as 1700–1800 °C,¹ while those synthesized by various wet-chemical routes need a typical densification temperature of 1400–1600 °C.^{3–6}

To achieve a further decrease in the densification temperature and an easier microstructure control of the sintered body, we have tried the production of 20REDC (RE = La, Nd, Sm, Gd, Dy, Y, Ho, Er, and Yb) powders via carbonate coprecipitation using ammonium carbonate as the precipitant. In a previous paper,⁷ detailed characterization of the powders has been made and one of the most important conclusions drawn is that the ionic radius of the dopant has appreciable effects on powder properties, including particle morphology, agglomeration state, and the rate of crystallite coarsening. Though exhibiting the highest rate of crystallite growth upon calcination, the 20SmDC sample has an average crystallite size of only ≈34 nm at 900 °C. Therefore, high reactivity is expected from these carbonate-derived oxide solid solutions. In this paper, we investigate the densification behavior of these 20REDC materials.

Experimental Section

Compaction and Sintering. Powders for sintering were first dry-pressed manually (≈10-MPa pressure) into cylinders with a diameter of 6 mm and a length of 4–6 mm in a tungsten carbide die and then isostatically pressed to 200-MPa pressure. The densification behavior of powder compacts was investigated in air up to 1500 °C by means of constant-rate-of-heating (CRH) sintering performed on a thermal mechanical analyzer (Model TMA 1700, Rigaku, Tokyo, Japan) with a heating rate of 10 °C/min and a cooling rate of 20 °C/min. The sintered density, ρ , at any temperature can then be determined from the green density ρ_0 and the measured linear shrinkage $\Delta L/L_0$ using the equation

$$\rho = \rho_0 / (1 - \Delta L/L_0)^3 \quad (1)$$

where L_0 is the initial sample length and $\Delta L = L_0 - L$, where

* To whom correspondence should be addressed: Sintered Materials Research Group, Advanced Materials Laboratory, National Institute for Materials Science, Namiki 1-1, Tsukuba, Ibaraki 305-0044, Japan. Fax: +81-(0)298-52-7449. Tel.: +81-(0)298-51-3354 (ext. 2247). E-mail: LL.Jiguang@nims.go.jp.

[†] Present name: Advanced Materials Laboratory, National Institute for Materials Science.

(1) Kudo, T.; Obayashi, H. *J. Electrochem. Soc.* **1975**, *122*, 142.
 (2) Steele, B. C. H. *Solid State Ionics* **1984**, *12*, 391.
 (3) Duran, P.; Moure, C.; Jurado, J. R. *J. Mater. Sci.* **1994**, *29*, 1940.
 (4) Huang, K.; Feng, M.; Goodenough, J. B. *J. Am. Ceram. Soc.* **1998**, *81*, 357.
 (5) Higashi, K.; Sonoda, K.; Ono, H.; Sameshita, S.; Hirata, Y. *J. Mater. Res.* **1999**, *14*, 957.
 (6) Yamashita, K.; Ramanujachary, K. V.; Greenblatt, M. *Solid State Ionics* **1995**, *81*, 53.

(7) Li, J. G.; Ikegami, T.; Mori, T.; Wada, T. *Chem. Mater.* **2001**, *13*, 2913.

L is the instantaneous sample length. The green density of a powder compact was calculated from its weight and geometric dimensions.

The conventional ramp-and-holding (RAH) sintering method was also used to study the densification of 20REDC solid solutions. In this case, powder compacts were heated in air in a tube furnace to the selected temperatures at 10 °C/min and then cooled to room temperature at 20 °C/min after soaking for 2 h. The final sintered densities were measured by the Archimedes method with distilled water as an intrusion medium. The relative density of a sintered body was obtained by dividing the measured true density by the theoretical density d_{th} of the material. Considering that rare-earth cations would occupy the Ce^{4+} sites¹ to form a solid solution of $Ce_{1-x}RE_xO_{2-x/2}$, the theoretical density d_{th} can be calculated according to

$$d_{th} = 4[(1-x)M_{Ce} + xM_{RE} + (2-x/2)M_O]/a^3N_A \quad (2)$$

where $x = 0.20$, a is the lattice constant of a 20REDC material at room temperature, N_A is the Avogadro constant, and M refers to the atomic weight.

X-ray Diffractometry (XRD) Analysis. The lattice constants of densified 20REDC materials were determined via XRD according to the method described previously.⁷ Fully dense 20REDC ceramics were crushed into powders (<80 mesh) using a zirconia mortar and pestle, and the resultant powders were then annealed at their respective sintering temperatures for 2 h to eliminate any possible strains induced by crushing. When necessary, the crystallite sizes of calcined oxide powders were determined via X-ray line broadening from the (422) diffraction of the ceria lattice.

Particle Morphology and Microstructure Observation. Particle morphology of the 20REDC oxide powders and microstructure of the sintered bodies were observed via high-resolution scanning electron microscopy (HRSEM) (Model S-5000, Hitachi, Tokyo, Japan). For sintered bodies, the sample surface was polished to a 1- μ m finish with diamond paste and then thermally etched in air at a temperature of 50 °C lower than the sintering temperature for 1 h to reveal grain boundaries. The etched surface was then coated with a thin layer of gold for conductivity before observation. The sample preparation procedures before observation for powder samples are the same as those described previously.⁷

Results and Discussion

Sintering. The sinterability of a powder is mainly controlled by its particle/crystallite size or surface area, which provides the driving force for densification. However, other physical properties (such as the range of particle size distribution, particle shape, and agglomeration) affect the compaction uniformity of particles in the green body and hence influence the densification process of powder compacts.⁸ Besides, chemical inhomogeneities in the powder may also have significant consequences for sintering. For 20REDC solid solutions, such chemical inhomogeneities may arise from a wide distribution of particle size. Rahaman et al.⁹ observed by means of high-resolution transmission electron microscopy (HRTEM) and energy-dispersive X-rays (EDX) that the CeO_2 powder doped with 6 at. % of Mg^{2+} , Sc^{3+} , or Y^{3+} cations, which has a bimodal distribution of particle size, shows a significant difference in the dopant concentration between larger and smaller particles, with the concentration being significantly higher in the finer particles.

We have investigated the densification behavior of 20REDC solid solutions under CRH sintering conditions, using powders calcined at 700 °C for 2 h. For powders calcined at even lower temperatures, some difficulties were encountered during compaction due to the extremely fine particle size and hence the huge friction force upon consolidation. Furthermore, the resulted powder compacts sometimes crack upon heating due to the stresses, arising from rapid shrinkage, around microstructural inhomogeneities. For the 20REDC oxides calcined at 700 °C for 2 h, our previous paper⁷ showed that the powders doped with cations smaller than Nd^{3+} (0.1109 nm) are mainly composed of spherical particles of uniform size and good dispersion. The size of primary particles was estimated to be around 12 nm from HRSEM micrographs and via X-ray line-broadening analysis. The powders doped with La^{3+} and Nd^{3+} , in contrast, are made up of secondary agglomerates of fibrous primary particles. The fibrous particles in 20LaDC are ≈ 0.1 – 0.3μ m in length and ≈ 15 nm in diameter, while the 20NdDC powder contains more rounded particles than 20LaDC and even its fibrous particles show significantly lower aspect ratio. The crystallite sizes of 20LaDC and 20NdDC are ≈ 9 and ≈ 12 nm, respectively.

Figure 1 compares the densification behaviors of 20REDC powders calcined at 700 °C under the CRH sintering conditions, with the green densities of powder compacts indicated in the figure. To maintain clarity, the results are presented as two parts, and the shrinkage curve of 20DyDC was re-plotted in Figure 1b for an easier comparison. It can be seen from Figure 1 that all these solid solutions behave like single compounds upon densification, without any additional expansion or contraction induced by solid-solution formation, chemical reaction, or solute redistribution observed. This is attributable to the uniform particle size and high chemical homogeneity. The present result is in contrast with those of Rahaman et al.⁹ and Duran et al.³ obtained from the 20YDC and 8GdDC powders synthesized by hydrothermal treatment and oxalate coprecipitation, respectively. In the latter two cases, severely depressed densification, due to solid-solution formation and/or solute redistribution among particles, was clearly identified on the shrinkage curves. Figure 1 shows that rapid shrinkage starts from the calcination temperature (700 °C) for each powder, but the temperature at which nearly full densification is reached varies significantly. The powders doped with smaller cations (Sm, Gd, Dy, Y, Ho, Er, and Yb) exhibit excellent sinterability and can be fully densified up to a very low temperature of ≈ 1100 °C at a constant heating rate of 10 °C/min. For the 20NdDC and 20LaDC powders, higher temperatures of ≈ 1200 and ≈ 1400 °C, respectively, are necessary for a nearly full densification.

The large difference in the densification temperature among these 20REDC oxides cannot be explained from the viewpoint of green density of the powder compact, which does not differ significantly. Obviously, the 20LaDC and 20YbDC powders exhibit very similar green densities upon consolidation but quite different densification temperatures upon sintering. Densification is a process of pore removal, and hence the pore structure in the green compact has dramatic effects on

(8) Lange, F. F. *J. Am. Ceram. Soc.* **1989**, *72*, 3.

(9) Rahaman, M. N.; Zhou, Y. C. *J. Euro. Ceram. Soc.* **1995**, *15*, 939.

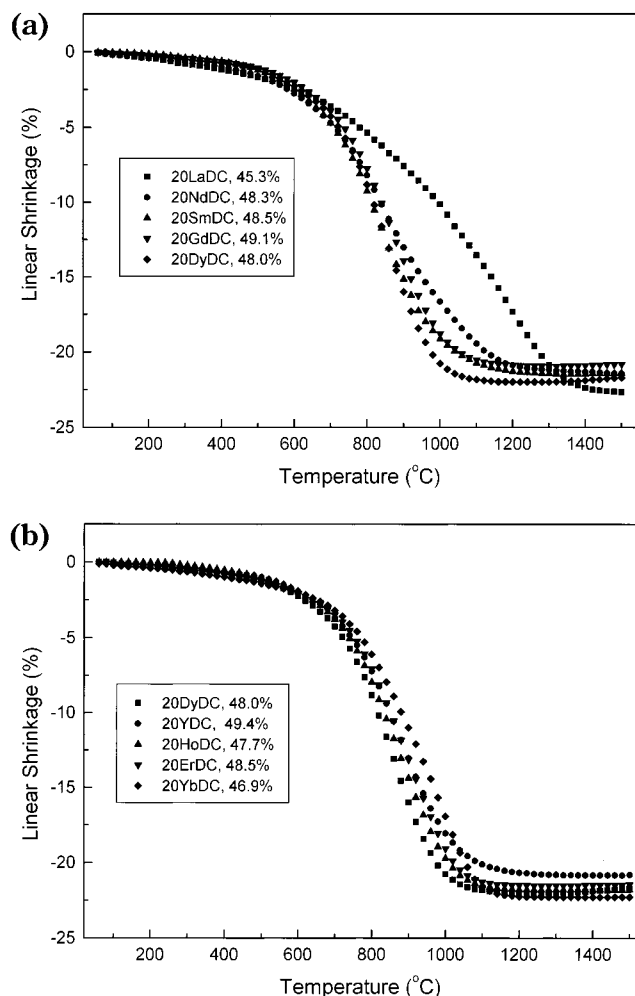


Figure 1. Densification behaviors of 20REDC oxides calcined at 700 °C under CRH sintering conditions. The heating and cooling rates are 10 and 20 °C/min, respectively. The green densities of powder compacts are indicated in the figure.

sintering. Green density, however, cannot reflect the pore structure. Green compacts of similar green densities may differ significantly in their pore structures when powders with different characteristics (particle size, size distribution, particle shape, and agglomeration) are used for compaction. The pores in a green compact can be viewed as an interpenetrating network with each pore defined by its neighboring particles. The number of neighboring particles is termed as the coordination number of the pore (N).⁸ Lange^{8,10} analyzed the process of pore elimination and found that although all the pores in the green body shrink, only those with a coordination number less than a critical value ($N \leq N_c$) disappear by sintering. Pores with $N > N_c$ shrink to an equilibrium size and are finally removed by grain growth at higher temperatures or during prolonged heating, through which their coordination numbers decrease to below N_c . The N_c value is related to the ratio of grain-boundary energy (γ_b) and surface energy (γ_s), that is, γ_b/γ_s .⁸ The N value of a pore in the green body, however, is closely related to the compaction uniformity of particles. The densification behavior of 20REDC oxides in this work is therefore considered to be mainly

controlled by particle morphology and the extent of agglomeration. Besides the ultrafine particle size, the low densification temperature of 20REDC (RE = Sm, Gd, Dy, Y, Ho, Er, and Yb) oxides is mainly benefited from the spherical particle morphology, narrow size distribution, and nonagglomeration, which ensures a high compaction uniformity of particles in the green body and a narrow distribution of the N value (few pores with $N > N_c$). For the 20LaDC and 20NdDC powders, the presence of aggregates and nonspherical particle morphology will cause nonuniform compaction of particles in the green body, and hence a wide distribution of the N value, resulting in higher temperatures for densification.^{8,10,11} The 20NdDC powder exhibits a higher densification rate than 20LaDC mainly due to its lower aspect ratio of particles and less agglomeration.

Calcination temperature affects particle morphology and the sinterability of 20REDC oxides. We select here 20SmDC, 20YbDC, and 20LaDC as representatives to discuss the influence of calcination temperature. These three samples were chosen for the following reasons considering the morphology of powders calcined at 700 °C and the rate of crystallite coarsening:⁷ (1) 20SmDC consists of rounded discrete particles and shows the highest rate of crystallite coarsening; (2) 20YbDC is similar to 20SmDC in particle morphology but exhibits a slow coarsening rate secondary only to 20LaDC; and (3) 20LaDC is fibrous in particle shape and shows the slowest rate of crystallite growth. Figures 2 and 3 exhibit the particle morphologies of 20SmDC and 20YbDC powders calcined up to 1000 °C, respectively. It can be seen that considerable crystallite coarsening occurred at these higher calcination temperatures. Besides, the particles gradually became faceted with increasing calcination temperature, indicating a gradual increase in crystallinity. All these powders show good dispersion, so uniform compaction of particles in the green bodies can be expected. Figure 4 shows the morphologies of 20LaDC powders calcined up to 1000 °C. Increasing the calcination temperature caused the secondary agglomerates in the powder to gradually collapse into discrete particles of lower aspect ratio. Fibrous particles are no longer observed in the powder calcined at 1000 °C and the particles show faceted morphologies. These changes in powder morphologies are expected to affect the compaction uniformity of particles in the green body and hence the densification behavior of 20LaDC oxides.

Figure 5 shows densification behaviors of 20SmDC, 20YbDC, and 20LaDC powders calcined at various temperatures, with the green densities of powder compacts indicated in the figure. As a general trend, the powder calcined at a higher temperature shows a higher onset temperature of rapid densification due to crystallite growth and reactivity loss. For 20SmDC (Figure 5a), increasing the calcination temperature from 700 to 1000 °C caused an $\approx 10\%$ increment in the green density, mainly due to crystallite coarsening (Figure 2). Crystallite growth, however, significantly lowers the sinterability of the powder, as predicted by Herring's scaling law.¹² Though the powder calcined at 800 °C (≈ 22 nm) still shows good reactivity and can be fully densified up

(10) Lange, F. F. *J. Am. Ceram. Soc.* **1984**, *67*, 83.

(11) Rajendran, S. *J. Mater. Sci.* **1994**, *29*, 5664.

(12) Herring, C. *J. Appl. Phys.* **1950**, *21*, 301.

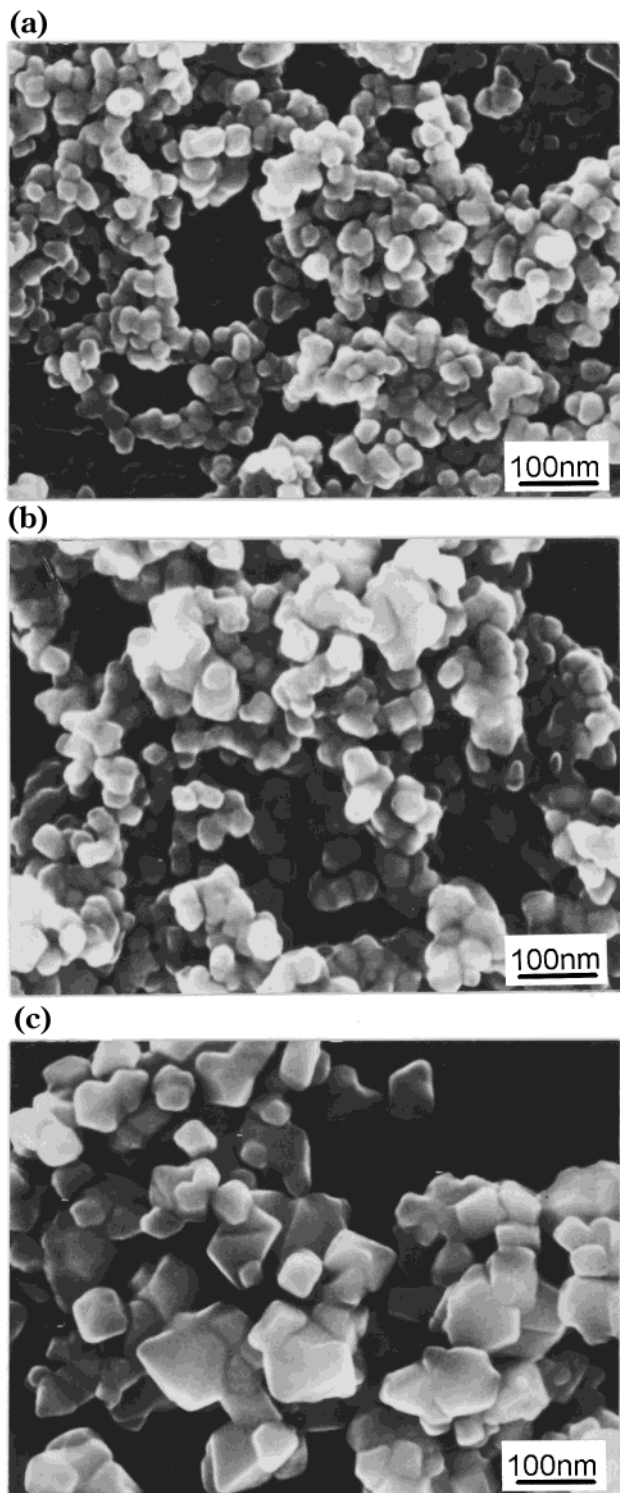


Figure 2. HRSEM micrographs showing particle morphologies of the 20SmDC powders calcined for 2 h at (a) 800, (b) 900, and (c) 1000 °C.

to a relatively low temperature of ≈ 1250 °C, calcining to 900 °C (≈ 34 nm) caused considerable reactivity loss and the powder has to be densified at a much higher temperature of ≈ 1400 °C. The powder calcined at 1000 °C (≈ 98 nm), however, becomes “nonsinterable”, and the final relative density reached at 1500 °C is only $\approx 92\%$, as calculated according to eq 1. Figure 5b shows the densification behaviors of 20YbDC powders calcined at various temperatures. Due to its slower rate of crystallite coarsening compared with 20SmDC, the green

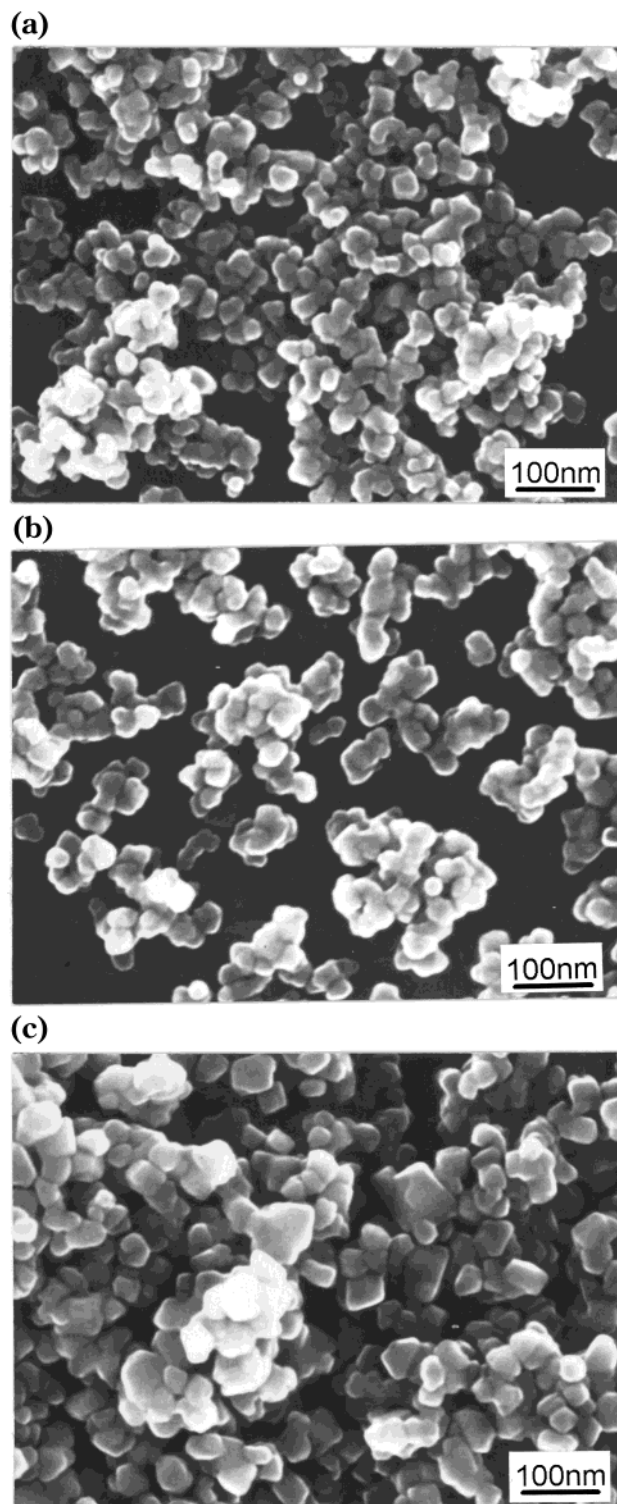


Figure 3. HRSEM micrographs showing particle morphologies of the 20YbDC powders calcined for 2 h at (a) 800, (b) 900, and (c) 1000 °C.

density increased only $\approx 4\%$ by raising the calcination temperature to 1000 °C. The powders calcined up to 900 °C (≈ 21 nm) exhibit good sinterability and can be fully densified up to ≈ 1250 °C. Compared with 20SmDC, the 20YbDC powder calcined at 1000 °C shows a much finer average crystallite size (≈ 46 nm) and can be fully densified up to ≈ 1440 °C due to its higher reactivity. The densification behaviors of 20LaDC oxides calcined at various temperatures are given in Figure 5c. At the same calcination temperature of 1000 °C, the 20LaDC

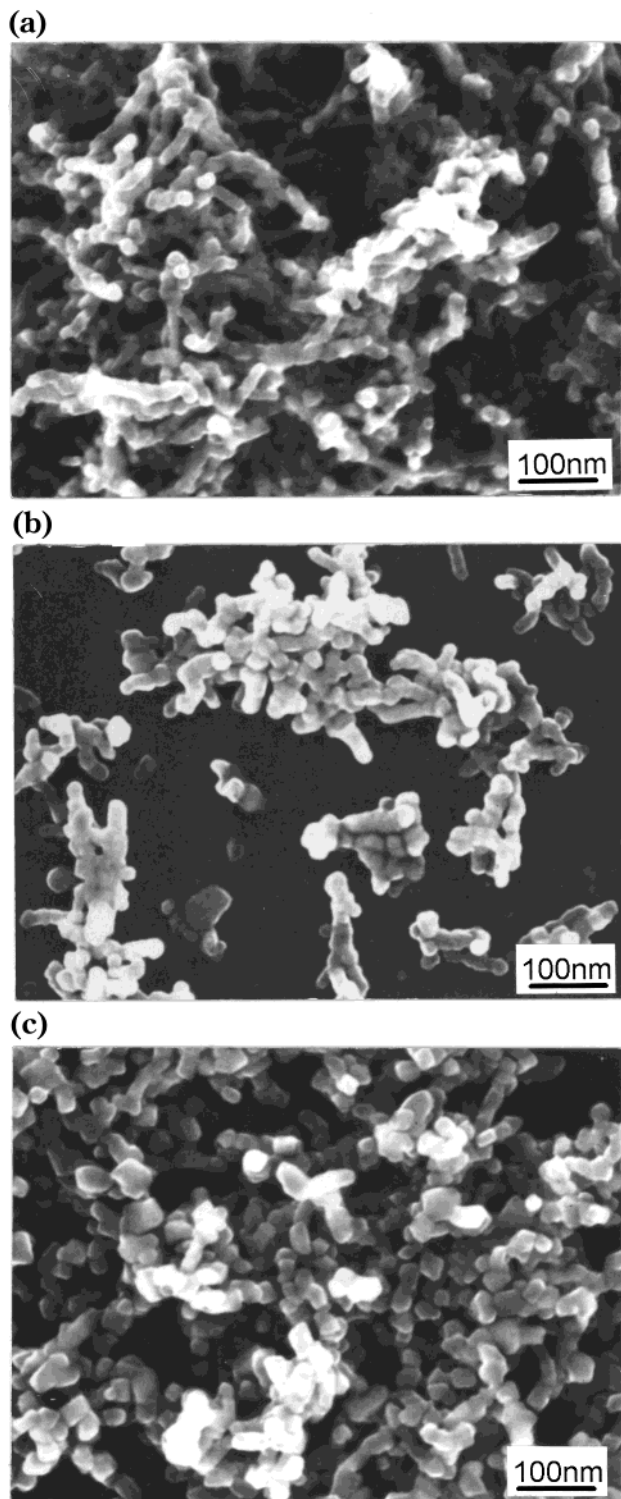


Figure 4. HRSEM micrographs showing particle morphologies of the 20LaDC powders calcined for 2 h at (a) 800, (b) 900, and (c) 1000 °C.

powder shows a lower green density than 20SmDC and 20YbDC, mainly due to its smaller crystallite size (≈ 30 nm). In contrast to 20SmDC and 20YbDC, the densification of 20LaDC powders shows a quite different dependence on the calcination temperature. It can be seen that all the powders calcined up to 1000 °C can reach a nearly full densification at the same temperature of ≈ 1400 °C. Besides, increasing the calcination temperature tends to enhance the densification rate of

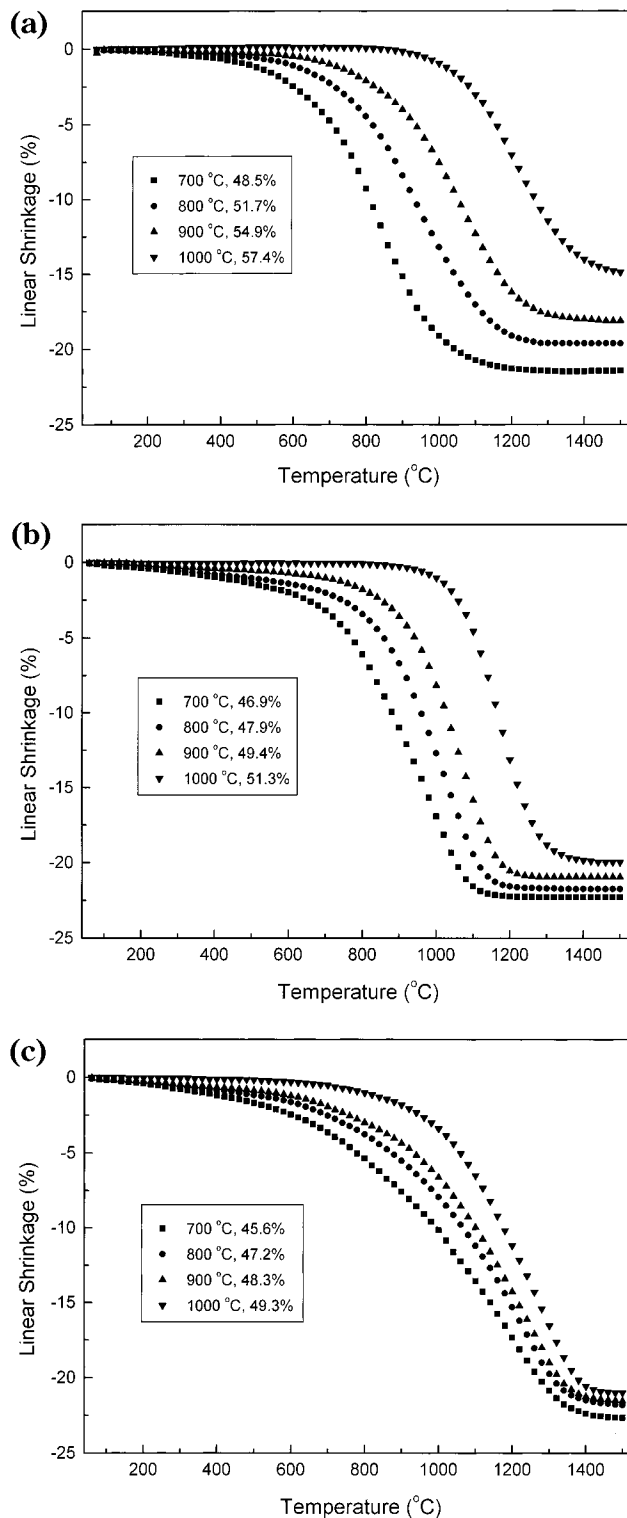


Figure 5. The effect of calcination temperature on the densification of 20REDC oxide solid solutions with (a) 20SmDC, (b) 20YbDC, and (c) 20LaDC. The heating and cooling rates for sintering are 10 and 20 °C/min, respectively. The green densities of powder compacts are indicated in the figure, along with the calcination temperature of the powder.

powder compacts. This phenomena can be explained from two aspects: (1) the powders calcined at high temperatures, such as 1000 °C, still possess high reactivity due to the very slow rate of crystallite growth (crystallite size ≈ 30 nm at 1000 °C), and (2) the secondary agglomerates in the powder gradually collapse into discrete particles of lower aspect ratio (Figure

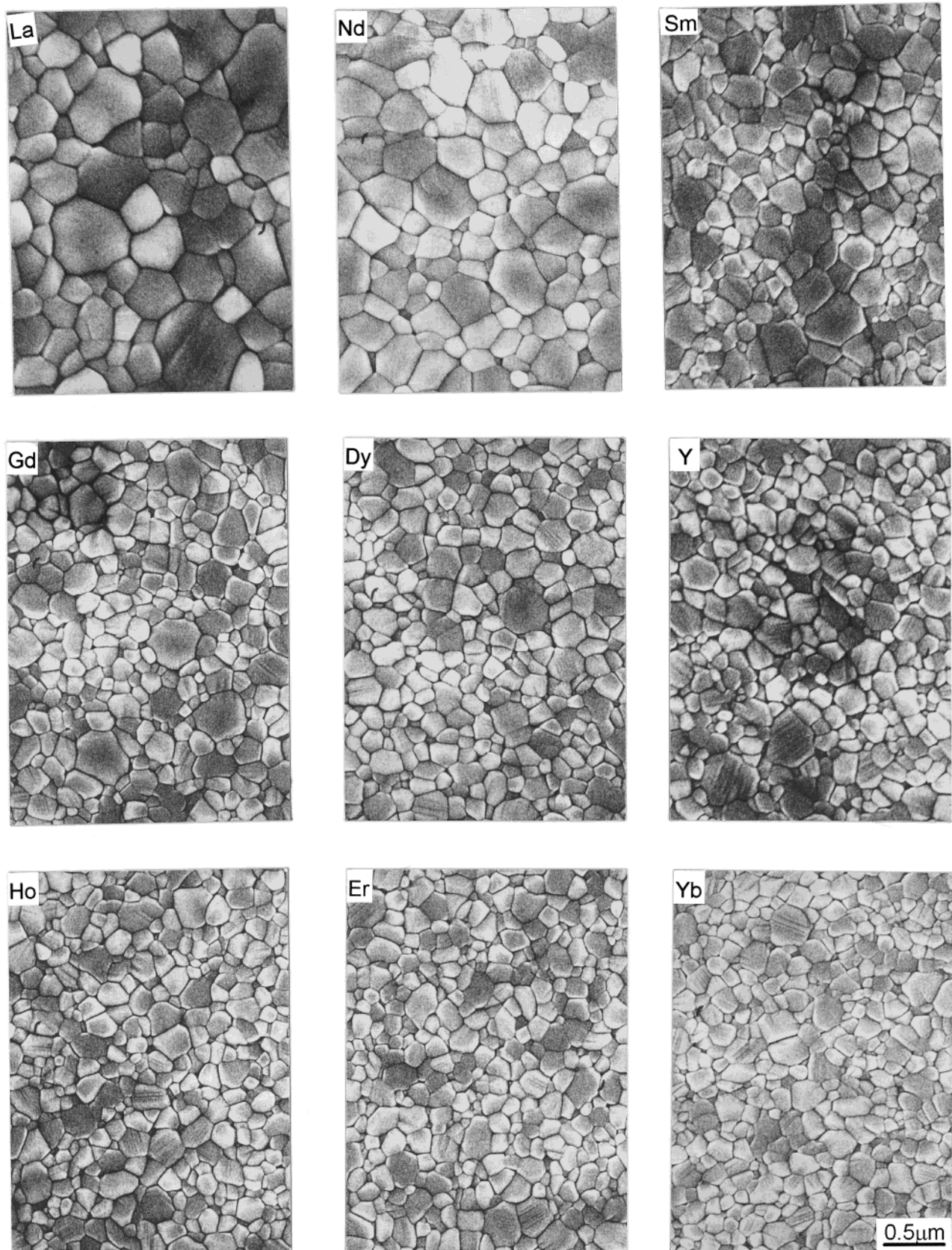


Figure 6. HRSEM micrographs showing microstructures of the densified 20REDC ceramics. The sintering temperature is 1250 °C for 20LaDC, 1150 °C for 20NdDC, and 1100 °C for the rest. The residence time is 2 h for each case. The dopants are indicated in the corresponding pictures, and the scale bar for 20YbDC is applicable to other materials.

4) with increasing calcination temperature, beneficial to a more uniform compaction of particles in the green body.

Figure 6 shows microstructures of the 20REDC ceramics densified by the RAH sintering method using powders calcined at 700 °C for 2 h. The sintering

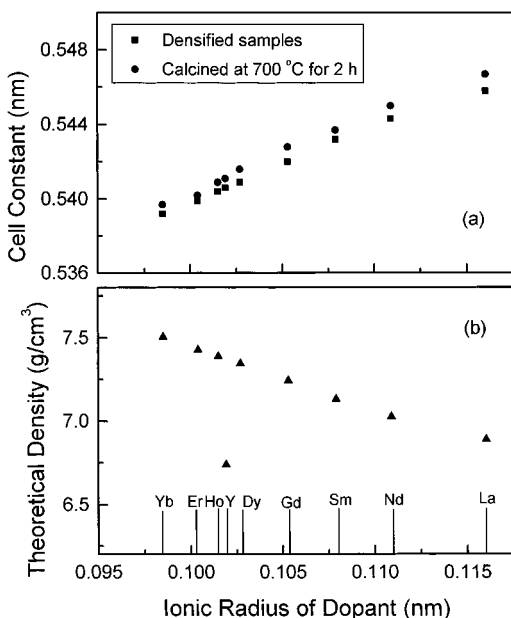


Figure 7. Lattice parameters (a) and theoretical densities (b) of the 20REDC solid solutions, as a function of the ionic radius of the dopant.

temperature is 1250 °C for 20LaDC, 1150 °C for 20NdDC, and 1100 °C for the rest. The residence time for sintering is 2 h for each case. These sintering temperatures were estimated from the shrinkage curves shown in Figure 1 to ensure full densification under the RAH sintering conditions. Though the densification temperature of 20LaDC is the highest in this work, it is still at least 150 °C lower than those reported for 20REDC oxides.^{3–6} It can be seen from Figure 6 that all the materials show uniform microstructures and have very few residue pores. The average grain size is $\approx 0.25 \mu\text{m}$ for 20LaDC, $\approx 0.2 \mu\text{m}$ for 20NdDC, and $\approx 0.15 \mu\text{m}$ for the rest, as determined by the linear intercept method. These fine microstructures are expected to improve the mechanical properties of 20REDC materials. Better mechanical property is important to 20REDC electrolytes, as they are used in the form of thin films or sheets in a SOFC apparatus.

Figure 7a shows the lattice constants of these densified 20REDC materials, and the data⁷ taken from powders calcined at 700 °C were included for comparison. The lattice parameters for the calcined powders are

slightly larger than those for the fully densified materials. This may be attributable to the much higher surface-to-volume ratio of powders compared with densified materials. In oxide particles, the chemical bonds have a directional character, and at the outer surface of each particle, there would be unpaired electronic orbitals, which would repel each other.¹³ This contribution from the surface layer increases with decreasing particle size and leads to larger values of the lattice parameter than in the bulk. Figure 7b gives the theoretical densities of 20REDC materials calculated according to eq 2, using lattice parameters taken from densified samples. The low theoretical density of 20YDC is due to the small atomic weight of yttrium. The 20REDC materials shown in Figure 6 are all >99.5% dense, as calculated by dividing their true densities measured by the Archimedes method with their respective theoretical densities.

Conclusions

The densification behavior of $Ce_{0.8}RE_{0.2}O_{1.9}$ (RE = La, Nd, Sm, Gd, Dy, Y, Ho, Er, and Yb) solid-solution powders, synthesized via coprecipitation using ammonium carbonate as the precipitant, has been investigated in air by means of constant-rate-of-heating and conventional ramp-and-holding sintering methods. The main conclusions are summarized as follows:

(1) Carbonate coprecipitation is a convenient method to synthesize well-sinterable rare-earth-doped ceria powders. At a calcination temperature of 700 °C, the $Ce_{0.8}RE_{0.2}O_{1.9}$ powders are highly reactive and can be sintered to >99.5% of the theoretical at very low temperatures of 1100–1250 °C. The resultant ceramics show uniform microstructures with ultrafine grain sizes of 150–250 nm.

(2) The densification behavior of $Ce_{0.8}RE_{0.2}O_{1.9}$ solid-solution powders is mainly influenced by the rate of crystallite coarsening, particle morphology, and the extent of agglomeration. The densification of $Ce_{0.8}La_{0.2}O_{1.9}$ powder, which requires the highest temperature (1250 °C) in this work, may be achieved at lower temperatures by synthesizing spherical-shaped, less-agglomerated powders.

CM010149P

(13) Ayyub, P.; Palkar, V. R.; Chattopadhyay, S.; Multani, M. *Phys. Rev. B* **1995**, *51*, 6135.